A quantitative model for the cooperative mechanism of human hemoglobin

(cooperativity/free energy coupling/protein interactions)

MICHAEL L. JOHNSON*, BENJAMIN W. TURNER†, AND GARY K. ACKERS†

*Department of Pharmacology, University of Virginia, Charlottesville, VA 22908; and †Department of Biology, The Johns Hopkins University, Baltimore, MD 21218

ABSTRACT   A quantitative model has been developed for the cooperative oxygenation of human hemoglobin. The model correlates the structural and energetic features of ligand-linked subunit interactions within the tetrameric molecule and the coupling of these interactions to the binding of oxygen and Bohr protons. Recent findings are incorporated regarding (i) the sites of regulatory energy change within the tetrameric molecule, (ii) the nature of the Bohr effect for tetramers and dimers, (iii) the fractional Bohr proton release at each stage of oxygenation, (iv) relative probabilities of binding to the α and β chains within the tetramer, and (v) an extensive data base recently obtained on the linked processes of oxygenation, proton binding, and subunit interactions [Chu, A. H., Turner, B. W. & Ackers, G. K. (1984) Biochemistry 23, 604–617]. Least squares minimization was used to evaluate from these data the free energies for the various processes. A special feature of the model lies in the synchronization of Bohr proton release with changes in quaternary structure. This leads to the striking prediction that a major fraction (as much as 30%) of tetramers are in the oxy quaternary structure after the first oxygen is bound. The model provides a rationale for the essential features of regulatory energy control, and it defines several kinds of additional information that are needed for a more complete understanding of the hemoglobin mechanism.

Cooperative oxygen binding in human hemoglobin is a classic example of the problem of relating structure to function in biological macromolecules. The appeal of hemoglobin as a system in which to study this problem stems in part from the facts that (i) the tetrameric molecule exhibits self-regulation by changing its affinity for oxygen at the four successive binding steps, (ii) structurally the hemoglobin molecule is relatively simple compared with other self-regulating macromolecular assemblies, and (iii) hemoglobin operates essentially as an equilibrium thermodynamic system in vivo, so that the biological processes of interest are purely thermodynamic in character—e.g., the changes in Gibbs free energies of the stepwise binding reactions. The structure–function problem is thus one of relating structural changes to thermodynamic changes and of understanding how these processes are influenced by interactions of the protein with small "regulatory" molecules such as protons, Cl^-, CO_2, and organic phosphates.

Much of the necessary structural information regarding the tertiary and quaternary changes that accompany oxygenation has been provided by extensive x-ray crystallographic studies, beginning with the classic work of Perutz and colleagues (1). The crystallographic results (cf. ref. 2) have been supplemented by structural studies in solution by extended

x-ray absorption fine structure (3), resonance Raman (4), and NMR (5) spectroscopy.

Equally important to an understanding of the cooperative mechanism is a knowledge of the sources and manifestations of free energy change that accompany the functional cycle of oxygenation–deoxygenation. We have carried out an extensive series of studies over the last 10 years aimed at resolving energetic aspects of the hemoglobin mechanism and of correlating the thermodynamic and structural information (cf. refs. 6–15). These studies, and work from other laboratories, have resulted in findings that impose stringent constraints on the nature of interactions responsible for cooperativity. In this paper we present a statistical thermodynamic model that incorporates these recent findings. (For other models of hemoglobin see refs. 11 and 16–23.)

An important requirement of structure–energy correlations in macromolecules is that comparably detailed information must exist in both areas for a meaningful correlation to be established. In the past, the structural analyses have provided an admirable wealth of detailed (atomic-level) information, whereas the corresponding development of energetic information has been severely lagging. Thus models based upon detailed structural assumptions—e.g., the Perutz mechanism (21, 22)—have only recently become amenable to critical tests (3–5, 12–14). An example is the detailed model of Szabo and Karplus (23), which we have now tested against the extensive sets of highly accurate pH-dependent oxygenation data recently obtained (15). We could find no reasonable set of values for that model's parameters capable of fitting the entire range of experimental data now available (see Addendum).

An appropriate base of information on hemoglobin does not presently exist for an adequate correlation between structural and energetic properties at the atomic level. As a result of recent studies, however, there is now a base of thermodynamic information that is sufficient to define the roles of pairwise intersubunit interactions in mediating cooperativity. The model we have developed has been formulated at this level, without any attempt to account for the detailed roles of the numerous pairwise atomic-level interactions that change throughout the molecule upon oxygenation. Our strategy has been to devise the simplest model that incorporates the presently available information with a minimum of ad hoc assumptions.

DEFINITIONS AND MODEL ASSUMPTIONS

Rationale. The major assumptions used in the model are all derived from, or supported by, experimental findings, briefly summarized here.

Structural and thermodynamic studies have shown that the hemoglobin tetramer is fundamentally a system of interacting dimers (designated $\alpha^1\beta^1$ and $\alpha^2\beta^2$) in which three pairwise intersubunit contacts are altered upon oxygenation:

$\alpha^1\beta^2$, $\alpha^2\beta^1$, and $\alpha^1\alpha^2$ (cf. refs. 2, 6, and 7). Topographically these may be represented by the diagram:
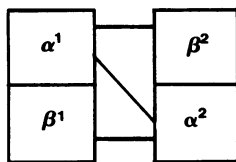
in which each line connecting a subunit pair represents a group of noncovalent interactions of various types—e.g., hydrogen bonds, ionic bonds (salt bridges), van der Waals interactions, and hydrophobic interactions. The β chains share no intersubunit contact in either the unligated or ligated states. The dissociated dimers bind oxygen noncooperatively (7, 15) but have a Bohr effect similar to that of isolated α and β chains (24). Upon binding of oxygen to a given subunit within the tetramer small changes in tertiary structure occur (2), and these are propagated into the $\alpha^1\beta^2$ intersubunit contact region of the molecule. The resulting local structure changes within this intersubunit contact region give rise to the free energies that constitute cooperativity (14). This regulatory energy is controlled by binding events at the heme sites. X-ray studies show that within each of the contacts $\alpha^1\beta^2$ or $\alpha^2\beta^1$ the ligation-induced structure changes occur primarily in two "subcontact" regions—the α_{FG}-β_C helix and the β_{FG}-α_C helix (2). Evidence from NMR studies (25) and thermodynamic work (26) indicates that oxygenation is accompanied by transitions involving more than two energetically significant structural forms; thus the changes in intersubunit contacts are not concerted [i.e., as in the Monod–Wyman–Changeux model (16)].

The model described in this paper does not distinguish between opposing views as to just which residues are responsible for the Bohr effect (cf. refs. 5, 21, 22, and 27–30). Rather it provides a unifying framework for understanding the relationships between Bohr proton release and the other molecular processes regardless of the exact source of the protons.

Whereas assembly of two deoxygenated $\alpha^1\beta^1$ dimers into a tetramer leads to a decrease in oxygen binding affinity, the assembly of a triliganded tetramer (from a doubly liganded dimer and a single liganded dimer) leads to an increased affinity for binding oxygen at the vacant site. This phenomenon is called *quaternary enhancement* (8, 9, 15).

Specific Assumptions. (*i*) A subunit may assume either of two tertiary forms. When oxygen is bound the subunit assumes the "ligated tertiary structure"; otherwise it has the "unligated tertiary structure." The free energy of binding an oxygen to a subunit (α or β) is defined to include the free energy of tertiary change for that subunit, thus incorporating the energetic contribution of the tertiary Bohr effect (assumption *vi-b* below).

(*ii*) Hemoglobin tetramers exist in two quaternary forms, which we designate the "deoxy quaternary state" and the "oxy quaternary state." The free energies of these states are defined relative to the free energy of oxygenated dimers, which are used as a reference species. The free energy difference between the oxy and deoxy states includes the free energy of the quaternary Bohr effect (assumption *vi-a* below).

(*iii*) When a tetramer is in the deoxy quaternary state, a ligated subunit suffers an unfavorable *free energy of quaternary enhancement*.

(*iv*) When a tetramer is in the oxy quaternary state, each unligated subunit suffers an unfavorable *free energy of quaternary enhancement*.

(*v*) Ligation-sensitive noncovalent interactions between pairwise subunit contacts $\alpha^1\beta^2$, $\alpha^2\beta^1$, and $\alpha^1\alpha^2$ are altered according to the following rules: (*a*) When either subunit of a pair is ligated, the intersubunit free energy assumes a new

value. (*b*) When both members of the pair are ligated, the ligation-sensitive interaction free energy vanishes. Values of these interaction energies may be different for the two quaternary forms.

(*vi*) The alkaline Bohr effect for tetramers is the sum of two components: (*a*) The *quaternary Bohr effect* is the change in protons bound that results from alteration of the structure upon going from deoxy to oxy quaternary states. (*b*) The *tertiary Bohr effect* is the change in protons bound that arises from structure changes within a subunit when ligated.

The assumptions incorporated into the model prescribe the 20 microscopic states of tetrameric hemoglobin as depicted in Fig. 1.

Definitions of Model Parameters.

δ_α, δ_β	Intrinsic free energy for oxygenation of α and β subunits in dimers and tetramers.
δ_{deoxy}, δ_{oxy}	Free energy to assemble oxygenated dimers into oxygenated tetramers in the deoxy and oxy quaternary states.
$\delta_{deoxy}^{\alpha\alpha}$, $\delta_{oxy}^{\alpha\alpha}$	Oxygenation-sensitive free energy of interaction between α^1 and α^2 in the deoxy or oxy quaternary state when neither chain is oxygenated.
$\delta_{deoxy}^{\alpha\beta}$, $\delta_{oxy}^{\alpha\beta}$	Oxygenation-sensitive free energy of interaction between α^1 and β^2 or α^2 and β^1 subunits when neither chain is oxygenated.
$\delta_{deoxy}^{\alpha\alpha K}$, $\delta_{oxy}^{\alpha\alpha K}$ $\delta_{deoxy}^{\alpha\beta}$, $\delta_{oxy}^{\alpha\beta}$	Analogous to the previous four parameters except that they pertain to interactions where one of the two subunits is oxygenated.
δ_{QE}	Free energy of quaternary enhancement.

QUANTITATIVE FORMULATION

Here we list the principal relationships used for "translation" of the model parameters into the model-independent thermodynamic parameters. The statistical thermodynamic methods we used have been described (12).

The equilibrium binding constants for i ligands reacting with unliganded tetramer are given by

$$K_{4i} = \frac{\xi_{4i}}{\xi_{40}}, \qquad [1]$$

where ξ_{4i} is the subsystem partition function for tetramers with i ligands bound

$$\xi_{4i} = \sum_j g_{ij} \exp(-G_{ij}/RT). \qquad [2]$$

In Eq. 2 G_{ij} is the free energy of configuration j with i ligands bound relative to the reference species—unliganded dimers. G_{ij} is the sum of all energetic contributions to a given state—i.e., the number of interactions of a given type times the free energy of that interaction, summed over each of the types of interactions. g_{ij} is the degeneracy of energy G_{ij}. R is the gas constant and T is the absolute temperature.

The probabilities of microscopic states among tetramers with i ligands bound are:

$$P_{ij} = \frac{g_{ij} \exp(-G_{ij}/RT)}{\xi_{4i}}. \qquad [3]$$

Relationships similar to those of Eqs. 1–3 hold for dimers. The equilibrium constant for dimer–tetramer assembly in the unliganded species is given by:

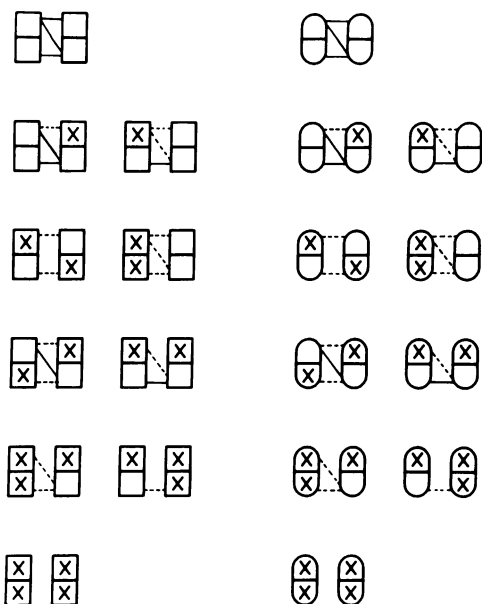$$^0K_2 = \frac{\xi_{40}}{(\xi_{20})^2}. \qquad [4]$$

FIG. 1. Allowed tetrameric states. Each state is represented by a pair of dimeric subunits ($\alpha^1\beta^1$ and $\alpha^2\beta^2$). Rectangular subunits denote the deoxy quaternary state and rounded subunits denote the oxy quaternary state. Ligation is represented by the presence of an X for each oxygen molecule bound. Horizontal lines represent subunit interactions $\alpha^1\beta^2$ and $\alpha^2\beta^1$. Diagonal lines correspond to $\alpha^1\alpha^2$ interaction. Solid lines denote interaction when neither subunit is ligated and the broken lines represent the altered interaction when one member of the pair is ligated.

Eq. 1–4 provide the necessary connection between the raw data and energetic parameters of the model since the former are described (6) by:

$$\overline{Y} = \frac{Z_2{}' + Z_4{}' \ [(Z_2 + 4^0 K_2 Z_4[P_t])^{1/2} - Z_2]/Z_4}{Z_2 + (Z_2 + 4^0 K_2 Z_4[P_t])^{1/2}} \quad [5]$$

where

$$Z_2 = 1 + K_{21}[X] + K_{22}[X]^2$$

$$Z_2{}' = K_{21}[X] + 2K_{22}[X]^2$$

$$Z_4 = 1 + K_{41}[X] + K_{42}[X]^2 + K_{43}[X]^3 + K_{44}[X]^4$$

$$Z_4{}' = K_{41}[X] + 2K_{42}[X]^2 + 3K_{43}[X]^3 + 4K_{44}[X]^4.$$

$[P_t]$ is the total protein concentration in terms of moles of heme. [X] is the molar oxygen concentration, and K_{2i} and K_{4i} are the product Adair constants for oxygen binding to dimers and tetramers, respectively (cf. ref. 6 for detailed definition and derivation of Eq. 5).

ANALYSIS OF EXPERIMENTAL DATA

The model was tested against the recent experimental data sets of Chu *et al.* (15) and of Mills and Ackers (9) consisting of oxygen binding isotherms measured as a function of hemoglobin concentration. Each data set was taken at a fixed pH (i.e., pH 7.4, 8.0, 8.5, 8.95) in 0.1 M Tris·HCl/0.1 M NaCl/1 mM Na₂EDTA at 21.5°C. For each pH a corresponding study had been conducted on the dimer–tetramer assembly in the unligated and fully oxygenated states (24). These data, in combination with the oxygen binding isotherms, were analyzed (15) to obtain the pH dependence for the various steps of the linkage between subunit assembly and oxygen binding by dimers and tetramers. From these results the numbers of protons released at each stage of oxygenation were determined. These are given in Table 1. The tetramer Bohr effect (over all four steps) was in close agree-

Table 1. Bohr protons released ($\Delta \bar{\nu}_{4i}$) upon stepwise oxygenation

pH	$\Delta \bar{\nu}_{41}$	$\Delta \bar{\nu}_{42} + \Delta \bar{\nu}_{43}$	$\Delta \bar{\nu}_{44}$	$\Delta \bar{\nu}_2$
7.40	0.64 ± 0.07	1.62 ± 0.27	0.05 ± 0.06	0.22 ± 0.12
8.00	0.38 ± 0.03	1.16 ± 0.12	0.05 ± 0.06	0.07 ± 0.05
8.50	0.16 ± 0.03	0.78 ± 0.11	0.05 ± 0.05	-0.05 ± 0.04
8.95	-0.03 ± 0.06	0.44 ± 0.23	0.05 ± 0.06	-0.16 ± 0.09

Errors are 65% confidence limits.

ment with the differential titration data of Antonini *et al.* (31).

We fit the raw experimental data points to the mathematical functions of the model by a nonlinear least squares procedure, described elsewhere (12, 32, 33). In carrying out the analyses we imposed the following constraints on the fitting process.

(*i*) For each pH, we assumed the experimentally determined dimer Bohr effect to be a measure of the tertiary Bohr effect. We therefore calculated the quaternary Bohr effect for tetramers at each oxygen binding step as the difference between numbers of protons released by the tetrameric species and the numbers released by the dimeric species. Then the fractional change in the resulting quaternary Bohr effect was taken as a measure of the fractional change in quaternary structure at each oxygenation step.

(*ii*) We constrained the ratio of probabilities of binding oxygen by the α and β chains to be 1.0 ± 0.05 in the range between zero and half-saturation of tetramers, in accord with the results of NMR determinations (34, 35).

(*iii*) At pH 7.4 the change in quaternary structure with fractional saturation of tetramers $\bar{Y}_4$ was constrained to be linear to within 5% between $\bar{Y}_4 = 0$ and $\bar{Y}_4 = 0.5$, in accord with results of NMR determinations (34).

(*iv*) We constrained the relative values of pairwise subunit interaction energies. For each quaternary state the ratio of the pairwise interaction energy when neither member of the pair is ligated to that when a single member is ligated is the same for both kinds of interaction $\delta^{\alpha\alpha}$ and $\delta^{\alpha\beta}$.

(*v*) The value chosen for δ_{QE} was based on experimental determinations (8, 9, 15).

RESULTS AND DISCUSSION

We found that the new model was capable of fitting the experimental data over the entire pH range on the basis of (*i*) comparison of the variance of fit with the variance found in determining the thermodynamic constant at each pH (15), (*ii*) randomness in the distribution of residuals to the best fit, (*iii*) cross-correlation between the fitted parameters, and (*iv*) comparison between values of the thermodynamic constants calculated by using the best-fit model parameters and the error limits of their values obtained from fitting the same data for the thermodynamic constants alone.

For all of the data sets analyzed it was possible to obtain fits in which the model parameters had physically reasonable values. Representative values are given in Table 2. The observed shifts by several kilocalories in quaternary interaction parameters (i.e., δ_{deoxy}) over a narrow pH range reflect the highly cooperative nature of the molecular transitions. These net energetic terms are undoubtedly the resultant of many larger interaction energies that mostly cancel.

On the basis of these analyses, we used the model to predict the populations of states for the various microscopic forms of the tetramer. Representative examples of the dominant states are given in Fig. 2 for the distributions at pH 7.4 and 8.5. We note that this model prescribes a major fraction (as much as 30%) of quaternary structure change upon binding of the first oxygen molecule. This distribution is a necessary correlate of the synchronization of Bohr proton release with quaternary structure change. Such a distribution of qua-

Table 2.   Values of model parameters

Model parameter	Value, kcal	
	pH 7.4	pH 8.5
$\delta_\alpha,\ \delta_\beta$	−8.3	−8.47
δ_{deoxy}	−4.1 ± 2	−10.6 ± 0.6
δ_{oxy}	−8.0 ± 0.1	−9.3 ± 0.1
$\delta^{\alpha\alpha}_{deoxy}$	1.4 ± 0.4	−2.0 ± 0.8
$\delta^{\alpha\alpha}_{oxy}$	−3.4 ± 0.4	−1.9 ± 0.3
$\delta^{\alpha\beta}_{deoxy}$	−5.6 ± 1.5	−0.4 ± 0.5
$\delta^{\alpha\beta}_{oxy}$	−2.2 ± 0.2	−1.3 ± 0.3
$\delta^{\alpha\alpha K}_{deoxy}$	0.7	4.2
$\delta^{\alpha\alpha K}_{oxy}$	0.3	−0.1
$\delta^{\alpha\beta K}_{deoxy}$	−3.1 ± 1.5	1.0 ± 0.3
$\delta^{\alpha\beta K}_{oxy}$	0.2 ± 0.1	0.0 ± 0.1
δ_{QE}	0.8	0.8

One kilocalorie = 4.18 kJ.

ternary transitions is in striking contradiction with earlier models, where the fractional quaternary change upon binding the first oxygen is insignificant. The classic allosteric model of Monod *et al.* (16) is a case in point. Analysis of the same data at pH 7.4 as in the present work yielded the result that less than 1% of singly ligated tetramers have an altered quaternary structure (11). The percentage contribution of quaternary structural forms is given in Fig. 3 as a function of ligation state and of total saturation for pH 7.4 and 8.5. While the trends are similar, a significant contribution of the oxy quaternary form to the unligated species is shown for pH 7.4 but not at pH 8.5. Conversely, a distinct contribution of the deoxy quaternary form to the fully ligated state is indicated by the analysis of the pH 8.5 data but not at pH 7.4. The effect through the oxygenation curve is shown in Fig. 3*B* where the same percentage contribution is plotted against extent of saturation.

Fig. 4 shows the relative contributions of α and β chains in the oxygenation process at pH 7.4 and pH 8.5. The contribution from α chains at pH 7.4 is greater than at pH 8.5 for all intermediate ligation states, most notably for the first, where virtually no binding is predicted at pH 8.5. The extent of the
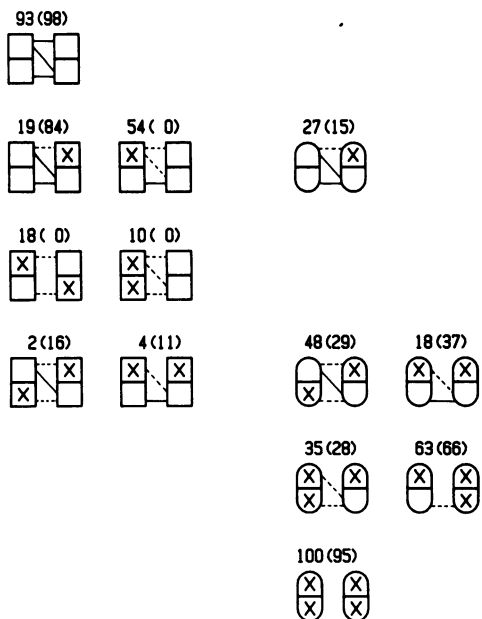

FIG. 2.   Population of significantly abundant states. All states with abundance greater than 5% are shown. Numbers on the left above each configuration refer to the actual percentages at pH 7.4. Numbers to the right in parentheses refer to percentages at pH 8.5.
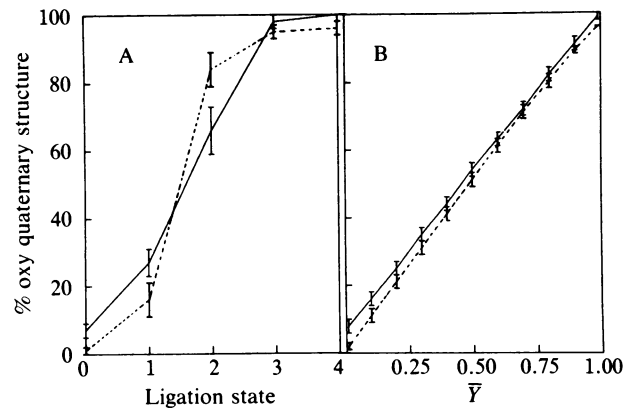

FIG. 3.   Relative contribution of oxy and deoxy quaternary forms upon ligation of tetramers as predicted by the model: Percentage contribution of oxy quaternary species for ligation states (*A*) and fractional saturation (*B*). Solid and broken lines correspond to typical analyses of pH 7.4 and 8.5 data, respectively. Bars indicate 65% confidence limits.

effect through the oxygenation curves is shown in Fig. 3*B*, where the same quantity is plotted against extent of saturation. The solid line (pH 7.4) is linear and indicates equal contribution of α and β chains, whereas the broken line is significantly curved and represents total contribution of α chain binding, which drops to as low as 40%. While this is illustrated only for the pH 8.5 data, this trend is exhibited in all data analyzed for pH values higher than 7.4.

The model that has been developed here correlates an immense body of experimental results and provides a framework for a more precise understanding of the regulatory mechanism in human hemoglobin. Consistency with a wide range of data is essential but does not, in itself, provide verification of a model. By contrast, tests that lead to altering a model's fundamental assumptions may contribute even more to the eventual understanding of mechanisms. The model developed here makes a number of predictions, as illustrated in Figs. 1–4. A number of these can be tested—e.g., by extended NMR studies of the fractional saturation of α and β chains (34, 35) and the fractional quaternary structure change (33, 34). Within the framework provided by this model, a more rigorous set of rules may be incorporated for the pairwise subunit interactions. There is now a very good prospect that such information will be obtainable from studies currently under way (26). The model can be extended further to incorporate the effects of 2,3-diphosphoglycerate, CO_2, and Cl^-
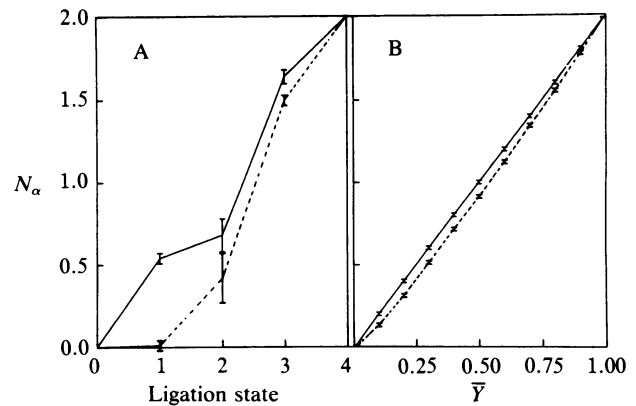

FIG. 4.   Predictions for the relative probabilities of binding oxygen molecules to α vs. β chains: Number of α chains with oxygen bound (N_α) for successive ligation states (*A*) and fractional saturation (*B*). Solid lines are from the analysis of pH 7.4 data and the dashed line to that of pH 8.5. Bars are 65% confidence limits.

Biophysics: Johnson *et al.*

Proc. Natl. Acad. Sci. USA 81 (1984)   1097

Table 3. Multiple minima of the Szabo–Karplus Model

Case	$-RT$ $\ln Q$	RT $\ln S$	RT $\ln K^\alpha$	RT $\ln K^\beta$	pK^α	pK^β	True variance $\times 10^5$
1	6.29	2.62	9.60	9.45	7.5	6.2	2.56
2	8.52	2.82	8.99	9.47	8.1	5.7	2.51
3	6.99	2.66	9.28	9.34	7.5	6.0	2.52
Model-independent experimental variance							2.52

Data of Mills *et al.* (7, 12) analyzed by methods described previously (12) to yield model parameter free energies in kcal: Q, for quaternary structure change; S for salt bridge formation; K^α and K^β, the intrinsic subunit oxygenation constants; pK^α and pK^β, the acid pK values for Bohr groups on α and β subunits, respectively. Model-independent parameters used in the fits were: $^0\Delta G_2 = -14.43$ and $\delta_\alpha = \delta_\beta = -8.405$ kcal (7).

binding, as well as mutant and chemically modified hemoglobins. These further developments and tests of the model will be described elsewhere.

ADDENDUM

We cannot be certain that no set of parameters could be found that would bring the Szabo–Karplus model into correspondence with the experimental data. The model is plagued by innumerable local minima, precluding a unique fit (12, 23). The best parameter set reported appears to be that presented very recently by Lee and Karplus (36) given in Table 3 (case 1). We have analyzed this parameter set by comparing it to the actual published data of Mills *et al.* (7, 12) rather than the simulated data used by Lee and Karplus (36). The resulting true sample variance is given in Table 3. We further tested the ability of this parameter set to predict the tetramer Bohr effect, and the results are shown as the solid line of Fig. 5. For comparison we show the experimental data points obtained by us (15) under identical buffer conditions and temperature as the pH 7.4 data (7). Differential titration data of Antonini *et al.* (31) are also shown. The two sets of experimental values, which virtually coincide, are in sharp disagreement with the prediction of the Szabo–Karplus model. Thus the analysis of the minimum recently reported by Lee and Karplus (36) reinforces the earlier conclusion (12) that the Szabo–Karplus model is incapable of accounting for the composite body of highly reliable experimental information presently available. To illustrate the problem of multiple minima we present in Table 3 two additional parameter sets that also provide excellent fits to the oxygenation data of Mills *et al.* (7) with physically reasonable constants. Like the
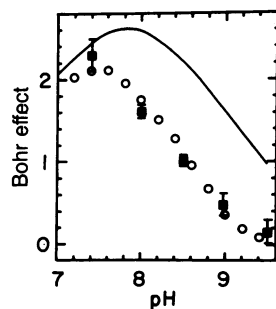

FIG. 5. Tetramer Bohr effect (number of protons released upon binding four oxygen molecules). ○, Data from differential titrations (31); ■, data from pH dependence of oxygenation data (15) determined under buffer and temperature conditions identical to those of Mills *et al.* (7). Error bars are 65% confidence limits. Solid line is the Bohr effect predicted by the Szabo–Karplus model with parameters reported by Lee and Karplus (ref. 36; see case 1 in Table 3).

Lee–Karplus result, none of these parameter sets, nor others we have found, satisfy the criteria of fitting oxygenation data with physically reasonable model parameters and also correctly predicting the Bohr effect.

1. Perutz, M. F., Muirhead, H., Mazzarella, L., Crowther, R. A., Greer, J. & Kilmartin, J. V. (1969) *Nature (London)* **222,** 1240–1243.
2. Baldwin, J. & Chothia, C. (1979) *J. Mol. Biol.* **129,** 175–220.
3. Eisenberger, P., Shulman, R. G., Kincaid, B. M., Brown, G. S. & Ogawa, S. (1978) *Nature (London)* **274,** 30–34.
4. Asher, S. A., Adams, M. L. & Schuster, T. M. (1981) *Biochemistry* **20,** 3339–3346.
5. Russu, I. N., Ho, N. T. & Ho, C. (1983) *Biochemistry* **22,** 5031–5043.
6. Ackers, G. K. & Halvorson, H. R. (1974) *Proc. Natl. Acad. Sci. USA* **71,** 4312–4316.
7. Mills, F. C., Johnson, M. L. & Ackers, G. K. (1976) *Biochemistry* **15,** 5350–5362.
8. Valdes, R. & Ackers, G. K. (1978) *Proc. Natl. Acad. Sci. USA* **75,** 311–314.
9. Mills, F. C. & Ackers, G. K. (1979) *Proc. Natl. Acad. Sci. USA* **76,** 273–277.
10. Ackers, G. K. (1980) *Biophys. J.* **32,** 331–346.
11. Ackers, G. K. & Johnson, M. L. (1981) *J. Mol. Biol.* **147,** 559–582.
12. Johnson, M. L. & Ackers, G. K. (1982) *Biochemistry* **21,** 201–211.
13. Flanagan, M. A., Ackers, G. K., Hanania, G. I. H. & Gurd, F. R. N. (1981) *Biochemistry* **20,** 7439–7449.
14. Pettigrew, D. W., Romeo, P. H., Tsapis, A., Thillet, J., Smith, M. L., Turner, B. W. & Ackers, G. K. (1982) *Proc. Natl. Acad. Sci. USA* **79,** 1849–1853.
15. Chu, A. H., Turner, B. W. & Ackers, G. K. (1984) *Biochemistry* **23,** 604–617.
16. Monod, J., Wyman, J. & Changeux, J.-P. (1965) *J. Mol. Biol.* **12,** 88–118.
17. Koshland, D. E., Nemethy, G. & Filmer, D. (1966) *Biochemistry* **5,** 364–385.
18. Weber, G. (1972) *Biochemistry* **11,** 864–878.
19. Weber, G. (1982) *Nature (London)* **300,** 603–607.
20. Herzfeld, J. & Stanley, E. (1974) *J. Mol. Biol.* **82,** 231–265.
21. Perutz, M. F. (1970) *Nature (London)* **228,** 726–734.
22. Perutz, M. F. (1970) *Nature (London)* **228,** 734–739.
23. Szabo, A. & Karplus, M. (1972) *J. Mol. Biol.* **72,** 163–197.
24. Chu, A. H. & Ackers, G. K. (1981) *J. Biol. Chem.* **256,** 1199–1205.
25. Miura, S. & Ho, C. (1982) *Biochemistry* **21,** 6280–6287.
26. Smith, F. R. & Ackers, G. K. (1983) *Biophys. J.* **41,** 415.
27. Kilmartin, J. V., Fogg, J. H. & Perutz, M. F. (1980) *Biochemistry* **19,** 3189–3193.
28. Perutz, M. F., Kilmartin, J. V., Nishikura, K., Fogg, J. H., Butler, P. J. G. & Rollema, H. J. (1980) *J. Mol. Biol.* **138,** 649–670.
29. Matthew, J. B., Hanania, G. I. H. & Gurd, F. R. N. (1979) *Biochemistry* **18,** 1919–1928.
30. Matthew, J. B., Hanania, G. I. H. & Gurd, F. R. N. (1979) *Biochemistry* **18,** 1928–1936.
31. Antonini, E., Wyman, J., Brunori, M., Fronticelli, C., Bucci, E. & Rossi-Fanelli, A. (1965) *J. Biol. Chem.* **240,** 1096–1103.
32. Johnson, M. L., Halvorson, H. R. & Ackers, G. K. (1976) *Biochemistry* **15,** 5363–5371.
33. Johnson, M. L. (1984) *Methods Enzymol.*, in press.
34. Viggiano, G. & Ho, C. (1979) *Proc. Natl. Acad. Sci. USA* **76,** 3673–3677.
35. Viggiano, G., Ho, N. T. & Ho, C. (1979) *Biochemistry* **18,** 5238–5247.
36. Lee, A. & Karplus, M. (1983) *Proc. Natl. Acad. Sci. USA* **80,** 7055–7059.